The Photonic Delay Technique for Phase Noise Measurement of Microwave Oscillators

Enrico Rubiola
*Université Henri Poincaré (*LPMIA *and* ESSTIN*), Nancy, France.*

Ertan Salik, Shouhua Huang, Nan Yu, and Lute Maleki
Jet Propulsion Laboratory, California Institute of Technology, Pasadena, CA, USA.
(Dated: 26th January 2004, 1025)

A photonic delay line is used as a frequency discriminator to measure the phase noise—hence the short-term frequency stability—of microwave oscillators. The scheme is suitable for electronic and photonic oscillators, including the opto-electronic oscillator, mode lock lasers, and other types of RF and microwave pulsed optical sources. The approach is inherently suitable for a wide range of frequency without reconfiguration, which is important for the measurement of tunable oscillators. It is also insensitive to a moderate frequency drift without the need for phase locking.

OCIS codes:

1. Introduction

The ever increasing demand for precision measurements in scientific and technological applications requires ultra-low noise, highly spectrally pure, and highly stable sources of reference signals. This is because phase, and equivalently frequency and time, are the most precisely measured physical quantities. Up until a decade ago, virtually all high performance reference oscillators operated in the RF region of the spectrum, and any higher frequency required multiplication steps that were cumbersome, and degraded the quality of the signal. In the past decade, optical techniques have overcome this obstacle, producing low noise sources for the millimeter wave and microwave frequency regimes. Photonic oscillators[1,2] and mode locked lasers[3,4] produce low noise references in the tens of GHz frequency domain, and advance many applications ranging from tests of fundamental physical laws, to optical A/D converts and radar. The advent of the femtosecond optical comb[5] has completed the missing link by extending the ability to measure and characterize optical frequencies through a comparison with the microwave sources.

As the quality of the reference signals have improved, the need for measurement systems capable of precisely characterizing them has also grown. Ultra-low noise measurement systems are difficult to implement and use, and the task of precise characterization of the noise of high performance reference sources is mostly relegated to metrological laboratories. This is because at the level of performance of advanced standards, the measurement system is required to operate at or near the fundamental noise limits. Every source of technical noise must be carefully identified, characterized, eliminated, or reduced. Precise measurements also typically require access to an ultra-low noise reference source, which is used to compare with the oscillator being characterized. In this conventional, heterodyne, approach the signals from the oscillator under test is mixed with that of the reference in a mixer, and the output at dc (zero frequency) is measured with a spectrum analyzer. The scheme requires that the frequency of the oscillator under test be at the same value as that of the high performance reference with which it is being compared. This is an additional constraint for the development of low noise sources, which may have a natural oscillating frequency different than that of the reference.

Because of this, the homodyne technique for characterization of the noise of the oscillator is also used. In this approach, the signal from the source is split into two branches, one of which is delayed for de-correlation before being mixed with the first branch. To achieve the required noise de-correlation over the (Fourier) frequency range of interest, the required delays are many microseconds long, and difficult to achieve with conventional electronic techniques. Here, again, optical techniques can provide new capabilities for overcoming this particular barrier. The use of long fiber delays provides a low loss and practical technique for use in homodyne schemes. A particularly desirable feature of this approach is its compatibility with optically generated microwave signals, which usually have an optical output and can be easily introduced into a fiber delay. Thus an effective scheme can be implemented, which is accessible to most research laboratories interested in the characterization of the noise of high performance oscillators.

Despite its great utility, the optically based noise measurement scheme is not widely known in the optics community. In this paper we aim at describing this approach, and provide a detailed analysis of its features and its limitations. We are interested in reference signal sources that have ultra-high spectral purity, and short term stability. Our approach is not suitable for measuring long

term stability, as needed, for example, for atomic clocks which must be characterized in the time domain with a completely different measurement system.

Since the subject of RF and microwave phase noise measurement is not necessarily a familiar one in the optics community, we begin our presentation with a discussion of the salient features of phase noise, which is also required for characterizing the time domain stability of reference sources. We will also present a description of the heterodyne phase noise measurement method to be compared with the homodyne technique. We provide a detailed analysis of the photonic delay line, and discuss the contributions of all sources of noise associated with various components in the measurement system. Finally, we apply the optical delay line to characterize the phase noise of a photonic oscillator that has a performance higher than commercial measurement instruments, such as spectrum analyzers, and thus requires a high performance test system.

2. Overview

Phase noise is described in terms of power spectral density $S_\varphi(f)$ of random phase fluctuations $\varphi(t)$, as a function of Fourier frequency f. This refers to the signal representation

$$v(t) = V_0 \left[1 + \alpha(t)\right] \cos\left[2\pi\nu_0 t + \varphi(t)\right] \quad . \tag{1}$$

Industry reports and specifications often use $\mathcal{L}(f)$, which is defined as $\mathcal{L}(f) = \frac{1}{2} S_\varphi(f)$. The amplitude noise $\alpha(t)$ and its spectrum are also of interest in many cases. An alternate quantity used to describe the frequency stability of oscillators, and closely related to $S_\varphi(f)$, is the two-sample (Allan) variance

$$\sigma_y^2(\tau) = \frac{1}{2} \overline{\left(\overline{y}_{k+1} - \overline{y}_k\right)^2} \quad , \tag{2}$$

where $\overline{y}_k$ and $\overline{y}_{k+1}$ are the fractional frequency fluctuation $y(t) = \frac{1}{2\pi\nu_0} \frac{d}{dt} \varphi(t)$ averaged on contiguous time intervals of duration τ, which is the measurement time.

A model that is found useful to describe the observed phase noise of oscillators is the power-law dependence of phase noise on the Fourier frequency

$$S_\varphi(f) = \sum_{i \le 0} b_i f^i \quad , \tag{3}$$

which includes the negative powers of f including f^0 (white phase noise) to at least f^{-4} (random walk of frequency), depending on the oscillator and on the observation time. Figure 1 shows the phase noise spectrum of an oscillator, and the Definitions of main terms of (3). Similar models also apply to the spectrum of frequency fluctuation $S_y(f)$ and to the Allan variance. Detailed discussions of phase noise and short-term stability are available in several references, amongst which we prefer the review paper[6] of Rutman, the CCIR report[7] 580-3,

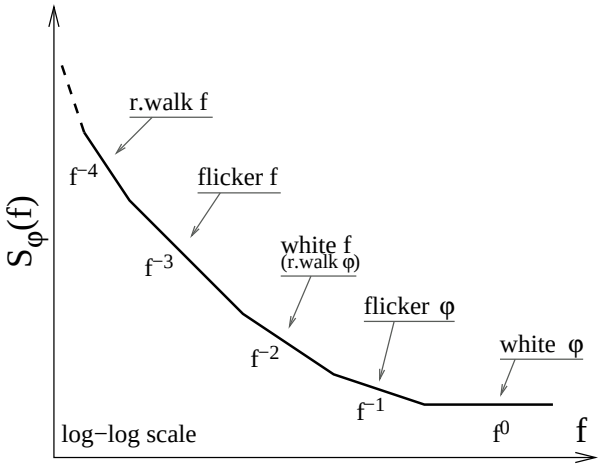

Figure 1. Oscillator phase noise.

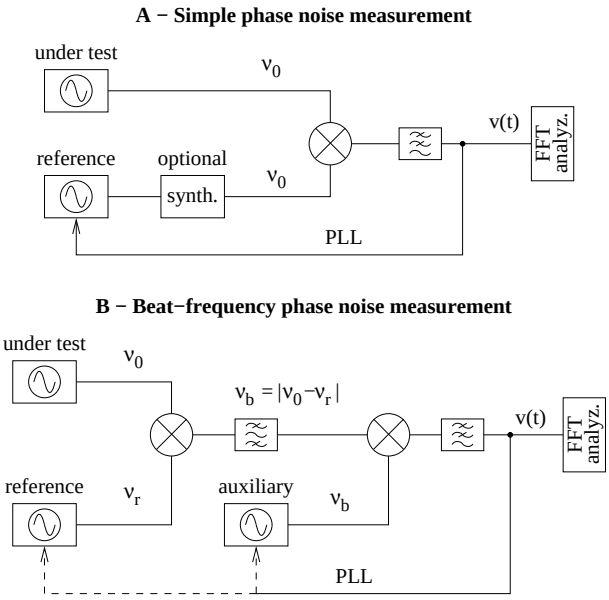

Figure 2. Usual schemes for the measurement of $S_\varphi(f)$.

a book edited by Kroupa[8], and the chapter 2 of Ref. 9. A standard[10] of the IEEE is also available.

Among the processes of Fig. 1, we are mainly interested in the flicker of frequency, which has a slope of f^{-3} in the log-log plot of $S_\varphi(f)$, and a constant variance, independent of τ.

For technical reasons, the direct measurement of $S_\varphi(f)$ by means of a fast Fourier transform (FFT) analyzer is preferable for short-term fluctuations, while the time-domain techniques for the direct measurement of $\sigma_y^2(\tau)$ are more suitable for slower fluctuations. The breakpoint is about $f = 1$ Hz, with an overlapping of 1–2 decades. As we are interested in short-term stability, it is therefore natural to explore the frequency-domain methods, even if the final result may be reported as $\sigma_y(\tau)$.

The basic method for the measurement of phase noise

in oscillators is shown in Fig. 2 A. The double balanced mixer, saturated at both inputs, works as a phase-to-voltage converter. The gain is typically in the range of 100–500 mV/rad, depending on the device and on power. A power of 5–10 mW is usually needed to saturate the mixer. The reference oscillator is phase-locked to the oscillator under test. When needed, a synthesizer makes the nominal frequencies equal. Whereas one may be inclined to use a loose loop and to measure phase noise at frequencies higher than the cutoff, a tight loop is often preferable because in this case the noise spectrum is multiplied by f^2. Thus, for example, the $1/f^3$ low-frequency spectrum (flicker of frequency) turns into $1/f$ (flicker of phase). As a result, the burden on the dynamic range of the FFT analyzer is strongly reduced. On the other hand, the tight loop relies upon the knowledge of the loop transfer function, which must be measured and accounted for in order to get $S_\varphi(f)$.

Two experimental problems are inherent in the scheme of Fig. 2 A. The first is that a synthesizer is needed if the oscillator under test does not oscillate at a convenient frequency. The needed resolution is often obtained at the expense of short-term stability, which limits the measurement. The second is that microwave leakage, unavoidable in some cases, artificially reduces the phase noise and makes the measurement results incorrect. In a different context, the same mechanism is exploited to reduce the oscillator noise by injection locking[11,12].

The beat method shown in Fig. 2 B solves the above problems. The main point is that there is some freedom in choosing the reference, which can be an oscillator with a frequency not far from ν_0, or a lower frequency oscillator followed by a frequency multiplier. In both cases, the short-term stability limitation of the microwave synthesizer is removed. The phase noise measurement takes place at the beat frequency ν_b in the high frequency (HF) region, where low noise synthesizers are available. Phase locking may be used with the reference or the auxiliary synthesizer, allowing more flexibility. In practice, ν_b is chosen to prevent any leakage from affecting the results. The scheme of Fig. 2 B offers the highest sensitivity. Yet the problem with it is that a suitable low-noise reference must be available, at a frequency ν_r not far from ν_0, say within 50 MHz. This can be a severe constraint if one plans to measure oscillators with natural outputs in the GHz range. Then, in some cases the loop gain is spread in a wide range. In short, this approach may be the only possible option for the most demanding applications, such as the case of the whispering gallery mode oscillators[13–15], but is difficult to design and to operate as a general purpose instrument.

We now turn our attention to the single-oscillator (homodyne) method, in which a frequency discriminator acts as the reference with which the oscillator under test is compared. Systems based on this technique have been in use since the early time of the oscillator metrology[16–18], and yet are much older; Pound used a discriminator to stabilize an oscillator[19]. A resonator of quality factor Q

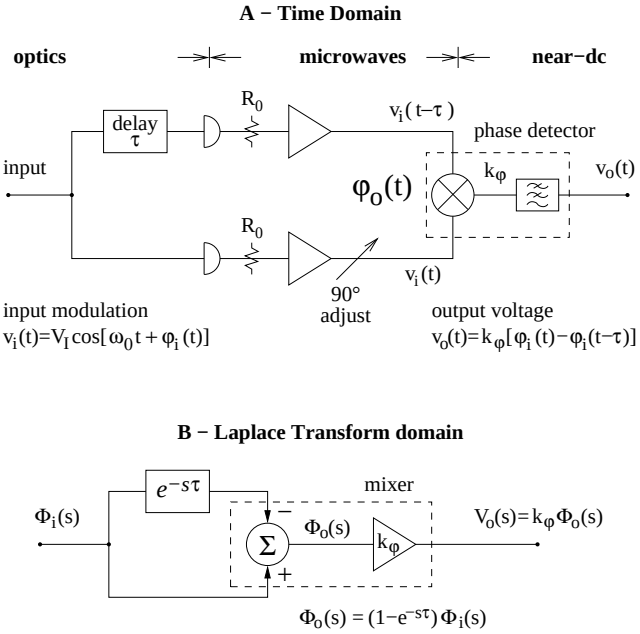

Figure 3. Delay-line homodyne method.

is a discriminator that turns frequency fluctuations $\delta\nu$ into phase fluctuations $\varphi = \delta\nu/2\nu Q$. For our purpose, a resonator tunable over a wide range would be necessary. Yet, the variable resonators do not have a sufficiently high stability and Q for the measurement of low-noise oscillators, and no significant progress has been made in this area since the early publications of references 16–18. A powerful alternative at our disposal is the photonic delay line, which will be analyzed in the following Sections.

In this homodyne approach, the discriminator gain is proportional to the delay, but an electrical delay line is not suitable at microwave frequencies because of high attenuation. For example, a UT-141 semirigid cable (3.5 mm diameter, PTFE insulated) has an insertion loss of some 0.8 dB/m at 10 GHz, which limits the achievable delay to about 100 ns (25 m). Even at lower frequencies, where a longer cable has a tolerable attenuation, it was necessary to use a correlation system with two independent delay lines and phase detectors[20,21] to overcome the high background noise that results from the short delay. Needless to say, the dual delay line system is cumbersome, complicated, and difficult to use.

Photonic technology offers a solution, since an optical fiber typically has a refractive index $n = 1.45$ and the attenuation is as low as 0.2 dB/km at the wavelength $\lambda = 1.55$ μm. Therefore, a 10 km coil exhibits a delay of 50 μs, in a reasonable size and weight (1×10^{-3} m^3 and 1 kg). A further advantage of the optical fiber, as compared to electrical cables, is that energy is perfectly confined. Thus, leakage, shielding and grounding are no longer a problem. Finally, the temperature stability of the index of refraction, thus of the delay, is $dn/dT \simeq 6.85\times10^{-6}$/K, which is more than one order of magnitude better than that of low thermal drift electrical cables.

3. Delay Line Theory

Figure 3 shows the principle of the delay-line measurement, and its equivalent in the Laplace transform domain. By inspection of Fig. 3,

$$\Phi_o(s) = H_\varphi(s)\Phi_i(s) \quad , \tag{4}$$

where $H_\varphi(s) = 1 - e^{-s\tau}$. Turning the Laplace transforms into power spectra, (4) becomes

$$S_{\varphi o}(f) = |H_\varphi(jf)|^2 S_{\varphi i}(f) \quad , \tag{5}$$

where

$$|H_\varphi(jf)|^2 = 4\sin^2(\pi f\tau) \quad . \tag{6}$$

The spectrum of frequency fluctuation $S_y(f)$ is related to $S_\varphi(f)$ through

$$S_y(f) = \frac{f^2}{\nu_0^2}\, S_{\varphi i}(f) \quad . \tag{7}$$

Combining (5) and (7), we get

$$S_y(f) = |H_y(jf)|^2 S_{\varphi i}(f) \quad , \tag{8}$$

where

$$|H_y(jf)|^2 = \frac{4\nu_0^2}{f^2}\ \sin^2(\pi f\tau) \quad . \tag{9}$$

Eq. (5) is used to derive the phase noise $S_{\varphi i}(f)$ of the oscillator under test. Alternatively, (7) is used to derive the frequency noise $S_y(f)$. We prefer $S_\varphi(f)$, independently of how the final results will be expressed, because the background noise of the instrument appears as $S_\varphi(f)$.

Figure 4 shows the transfer functions $|H_\varphi(jf)|^2$ and $|H_y(jf)|^2$ for $\nu_0 = 10$ GHz and $\tau_d = 10$ μs (2 km delay line), which is typical of our experiments. For $f \to 0$, it holds $|H_\varphi(jf)|^2 \sim f^2$. Fortunately, high slope processes such as flicker of frequency dominate in this region (see Fig. 1), which compensates $|H_\varphi(jf)|^2$. The phase noise measurement is therefore possible, providing the delay τ_d can be appropriately chosen. $|H_\varphi(jf)|^2$, as well as $|H_y(jf)|^2$, has a series of zeros at $f = \frac{n}{\tau_d}$, with integer $n \geq 1$. The experimental results are not useful in the vicinity of these zeros. At the beginning of our experiments we hoped to reconstruct the spectrum beyond the first zero at $f = \frac{1}{\tau_d}$ by exploiting the maxima at $f = \frac{2i+1}{2\tau_d}$ (integer $i \geq 1$). This turned out to be difficult. One problem is the resolution of the FFT analyzer, as the density of zeros increases on a logarithmic scale. Another problem is the presence of stray signals in the measured spectrum, which make unreliable the few data around the maxima. The practical limit is about $f = \frac{0.95}{\tau_d}$, where $|H_\varphi(jf)|^2 = -16$ dB, and at most some points around $f = \frac{3}{2\tau_d}$ between the first and second zeros.

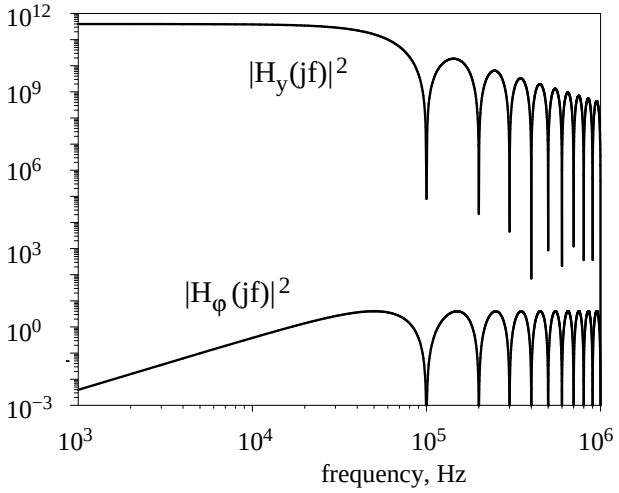

Figure 4. Transfer functions $|H_\varphi(jf)|^2$ and $|H_y(jf)|^2$ plotted for $\nu_0 = 10$ GHz and $\tau_d = 10$ μs.

4. Sources of Noise

The basic block for photonic phase noise measurements is shown in Fig. 3 A. In normal operation the random phase $\varphi(t)$ results from the fluctuations of the input frequency. In this section we analyze the sources of noise of the block, since $\varphi_o(t)$ is acquired from the noise of electrical and optical components.

The power $P_\lambda(t)$ of the optical signal is sinusoidally modulated at the microwave angular frequency ω_μ with a modulation index m

$$P_\lambda(t) = \overline{P}_\lambda\,(1 + m\cos\omega_\mu t) \quad . \tag{10}$$

Here, we use the subscripts λ and μ for 'light' and 'microwave', and the overline (as in $\overline{P}$) for the average. Eq. (10) is similar to the traditional AM of radio broadcasting, but optical power is modulated instead of RF voltage. In the presence of a distorted (nonlinear) modulation, we take the fundamental of the modulating signal, at ω_μ.

The detector photocurrent is

$$i(t) = \frac{q\eta}{h\nu_\lambda}\,\overline{P}_\lambda\,(1 + m\cos\omega_\mu t) \quad , \tag{11}$$

where $q = 1.602{\times}10^{-19}$ C is the electron charge, η the quantum efficiency of the photodetector, and $h = 6.626{\times}10^{-34}$ J/Hz the Planck constant. Only the ac term $m\cos\omega_\mu t$ of (11) contributes to the microwave signal. The microwave power fed into the load resistance R_0 is $\overline{P}_\mu = R_0\overline{i_{\rm ac}^2}$, hence

$$\overline{P}_\mu = \frac{1}{2}m^2 R_0 \left(\frac{q\eta}{h\nu_\lambda}\right)^2 \overline{P}_\lambda^2 \quad . \tag{12}$$

A. White Noise

The discrete nature of photons leads to the shot noise of power spectral density $N_s = 2qiR_0$ [W/Hz] at the

detector output. By virtue of (11),

$$N_s = \frac{q^2\eta}{h\nu_\lambda}\,\overline{P}_\lambda R_0 \tag{13}$$

In addition, there is the equivalent input noise of the amplifier loaded by R_0, whose power spectrum is

$$N_t = Fk_BT_0 \quad , \tag{14}$$

where F is the noise figure of the amplifier, $k_B = 1.38\times10^{-23}$ J/K the Boltzmann constant, and T_0 the temperature. The white noise $N_s + N_t$ turns into a noise floor $S_{\varphi 0} = (N_s + N_t)/P_\mu$ of $S_\varphi(f)$. Using (12), (13) and (14), the floor is

$$S_{\varphi 0} = \frac{2}{m^2}\left[2\frac{h\nu_\lambda}{\eta}\,\frac{1}{\overline{P}_\lambda} + \frac{Fk_BT_0}{R_0}\left(\frac{h\nu_\lambda}{q\eta}\right)^2\left(\frac{1}{\overline{P}_\lambda}\right)^2\right] \tag{15}$$

Eq. (15) holds for one arm of Fig. 3. As there are two independent arms, noise power is multiplied by two. In addition, it is convenient to *redefine* $\overline{P}_\lambda$ as the total input power, half of which goes to the detector input. Accounting for the two arms and changing $\overline{P}_\lambda \to \overline{P}_\lambda/2$, the phase noise floor of the entire block is

$$S_{\varphi 0} = \frac{16}{m^2}\left[\frac{h\nu_\lambda}{\eta}\,\frac{1}{\overline{P}_\lambda} + \frac{Fk_BT_0}{R_0}\left(\frac{h\nu_\lambda}{q\eta}\right)^2\left(\frac{1}{\overline{P}_\lambda}\right)^2\right] \tag{16}$$

Interestingly, the noise floor is proportional to $(\overline{P}_\lambda)^{-2}$ at low power, and to $(\overline{P}_\lambda)^{-1}$ above the threshold power

$$P_{\lambda,t} = \frac{Fk_BT_0}{R_0}\,\frac{h\nu_\lambda}{q^2\eta} \tag{17}$$

For example, taking $\nu_\lambda = 193.4$ THz (wavelength $\lambda = 1.55$ μm), $\eta = 0.6$, $F = 1$ (noise-free amplifier), and $m = 1$, we get a threshold power $P_{\lambda,t} = 689$ μW, setting the noise floor at $S_{\varphi 0} = 9.9\times10^{-15}$ rad^2/Hz (-140 dBrad^2/Hz).

When the mixer is used as a phase-to-voltage converter, saturated at both inputs, its noise is chiefly the noise of the output amplifier divided by the conversion gain k_φ. Assuming that the amplifier noise is 1.6 nV/$\sqrt{\text{Hz}}$ (our low-flicker amplifiers, input-terminated to 50 Ω) and that $k_\varphi = 0.1$ V/rad (conservative with respect to P_μ), the mixer noise is about 2.5×10^{-16} rad^2/Hz (-156 dBrad^2/Hz). In practice, the mixer noise can hardly approach the noise of the microwave amplifier because of the gain of the latter. The microwave gain, hidden in (16), is not a free parameter. Its permitted range derives from the need of operating the mixer in the saturation region, below the maximum power.

Figure 5 shows the noise floor $S_{\varphi 0}$ as a function of the total optical power for some reference cases.

B. Modulation Index

For a given CW laser power, the condition of maximum microwave power at the angular frequency ω_μ is that of a square-wave of the same frequency that switches symmetrically between 0 and $2\overline{P}_\lambda$. This is equivalent to replacing the term $m\cos\omega_\mu$ in Eq. (10) with a unity square-wave that flips between ±1. In our case the unity square-wave can be expanded in Fourier series truncated after the first term because the higher harmonics ($\omega = n\omega_\mu$, with integer $n \geq 2$) are not in the pass band of the microwave chain. Thus, the unity square-wave is replaced with sinusoid of angular frequency ω_μ and amplitude $4/\pi$. Therefore the square-wave modulation is equivalent to a sinusoidal modulation with a modulation index $m = 4/\pi \simeq 1.273$. $m > 1$ is no contradiction with the traditional modulation theory, it only means that the harmonic distortion is present.

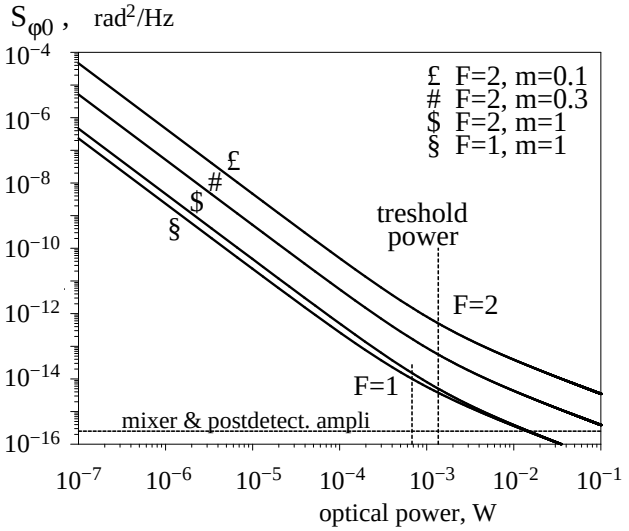

Figure 5. Noise floor as a function of the optical power. The treshld power depends on the noise figure F.

A more interesting case is that of the electro-optic modulator (EOM), which is used in virtually all photonic oscillators, and as the modulator in the experiments described below (section 6). The EOM transmission, as a function of the driving voltage $v(t)$, is

$$\mathcal{T} = \frac{1}{2} + \frac{1}{2}\sin\frac{\pi v}{V_\pi} \tag{18}$$

with V_π the half-wave voltage of the modulator. When the driving signal is $v(t) = V_p\cos\omega_\mu t$, the transmission becomes

$$\mathcal{T}(t) = \frac{1}{2}\left[1 + 2J_1\left(\frac{\pi V_p}{V_\pi}\right)\cos\omega_\mu t + \dots\right] \quad , \tag{19}$$

where J_1 is the first-order Bessel function of the first kind. Eq. (19) derives from 0-th term of the series expansion

$$\sin(z\cos\theta) = 2\sum_{k=0}^{\infty}(-1)^k J_{2k+1}\cos[(2k+1)\theta] \quad . \tag{20}$$

The neglected terms "..." of (19) are higher harmonics, of angular frequency $n\omega_\mu$, integer $n \geq 2$. They also ensure $0 \leq \mathcal{T} \leq 1$. Eq. (19) has the same form of Eq. (10),

hence the modulation index is

$$m = 2J_1\left(\frac{\pi V_p}{V_\pi}\right) \quad . \tag{21}$$

The maximum is $m \simeq 1.164$, which occurs at $V_p = 0.586\,V_\pi$.

In practice, the microwave power and the dc bias of the EOM are sometimes difficult to set and maintain at the maximum modulation index. This is due to the possibility for bias drift, and to the thermal sensitivity of the lithium niobate. Hence, we take $m = 1$ as the maximum, being aware that this may be somewhat optimistic.

C. Flicker Noise

The residual flicker noise derives from a number of causes for which there is no satisfactory theory. Nonetheless, based on experience and experimental facts, a model may be developed.

1. Amplifier

Phase flickering of amplifiers, as well as amplitude flickering, results from noise at near-dc frequency up-converted by the device nonlinearity. This is made evident by the simple observation that in the absence of a carrier the microwave spectrum at the amplifier output is white, i.e. constant over the entire bandwidth. Whereas a general theory does not exist, several experimental observations[22–24] suggest that different amplifiers based on a given technology tend to have about the same b_{-1} coefficient in (3), and that b_{-1} is nearly constant in a wide range of carrier frequency and power. The typical phase flickering of a "good" microwave amplifier operated well below the 1 dB compression point $P_{1\,\mathrm{dB}}$ is between $b_{-1} = 1{\times}10^{-11}$ and $b_{-1} = 2{\times}10^{-11}$. For example, b_{-1} of a commercial amplifier (Microwave Solutions MSH6545502) that we measured at 9.9 GHz is between $1.25{\times}10^{-11}$ and $2{\times}10^{-11}$ from 300 μW to 80 mW of output power. For this device, the 1 dB compression power is 160 mW.

In principle, the amplifier $1/f$ noise can be reduced by carrier suppression methods, in which only the noise sidebands are amplified. The difficulty of not having a clean reference with sufficient microwave power to pump the mixer has been recently solved[25]. Incorporating carrier suppression, which is well developed in the microwave domain[26], in a photonic oscillator has been demonstrated[27], but it is still a challenging task, and we are currently studying it further.

2. Mixer Noise

There are a number of microwave double-balanced mixers available that exhibit sufficiently low residual flicker. A conservative value for the flicker coefficient is $b_{-1} < 10^{-12}$. This makes the mixer noise negligible as compared to the amplifier. These low-noise mixers are available as commercial parts, without the need of individual selection. On the other hand, the double-balanced mixer needs to be saturated at both inputs in order to work properly as a phase detector. The power range is of a factor 10 centered around (±5 dB) an optimum power of 5–10 mW. At both sides out of that range, b_{-1} increases. Furthermore, at lower power the conversion gain (0.1–0.5 V/rad) drops suddenly. This is a consequence of the exponential $i(v)$ characteristics of the internal Schottky diodes.

3. Contamination from Amplitude Noise

Mixers are sensitive to the amplitude noise of the input signal. The output voltage v takes the form $v = k_\varphi\varphi + k_\alpha\alpha$, where $\alpha(t)$ is the amplitude fluctuation defined by Eq. (1). This results from the imperfect cancellation of the voltage across the internal diodes, due to diode differences and to the asymmetry of power splitting. In some cases we have measured k_φ/k_α as low as 5, while values of 10–20 are common. In spite of this, amplitude noise seldom represents a problem in microwave measurements, and at most turns into a small error in the measurement of $S_\varphi(f)$. Yet, in photonic systems the contamination from amplitude noise can be a serious problem because of the power fluctuation of some lasers and laser amplifiers, chiefly the EDFA. In the radiofrequency and microwave domain, Brendel[28], and later Gibel[29], suggest that the mixer can be operated at a point of zero sensitivity to amplitude noise. In practice this point occurs at a few degrees off the perfect quadrature, where the residual noise and the conversion gain of the mixer are not affected. That optimal point depends on the specific mixer sample, and on amplitude and frequency, for it must be determined experimentally in each case. Unfortunately, the Brendel offset method can not be used when a discriminator is inserted in one arm. This occurs because the null of amplitude sensitivity results from the equilibrium between equal and opposite sensitivities at the two inputs. The discriminator de-correlates the signals, hence the effect of a fluctuation of the input amplitude appears at the output twice, immediately and after the discriminator delay.

4. Noise of the Photonic Channel

The measurement of $1/f$ fluctuations in microwave photodetectors is a challenging problem, and has been reported previously only in a single instance[30]. In order to avoid the problem, we measured the noise of a photonic microwave channel, which consists of 1.55 μm laser diode (UTP CW-DFB-1550) followed by an EDFA (NuPhoton NP2000GB-23B-G23-NO-58-FPIS), an EOM (Lucent X2624C) and a photodetector (Discovery Semiconductor DSC30-1K, and Lasertron QDMH-3), the same components used in the final experiments. The measurement was carried out with a simplified version of the interferometric technique described in Ref. 26, measuring the fluctuation between the microwave input of the EOM and the microwave output of the photodetector at the frequency of 9.9 GHz. We swept the detection angle γ, without calibrating it. In this condition, the measured quantity is $\varphi\sin\gamma + \alpha\cos\gamma$, with arbitrary origin of γ. With a microwave power $P_\mu = 6.3$ μW (−22 dBm), the

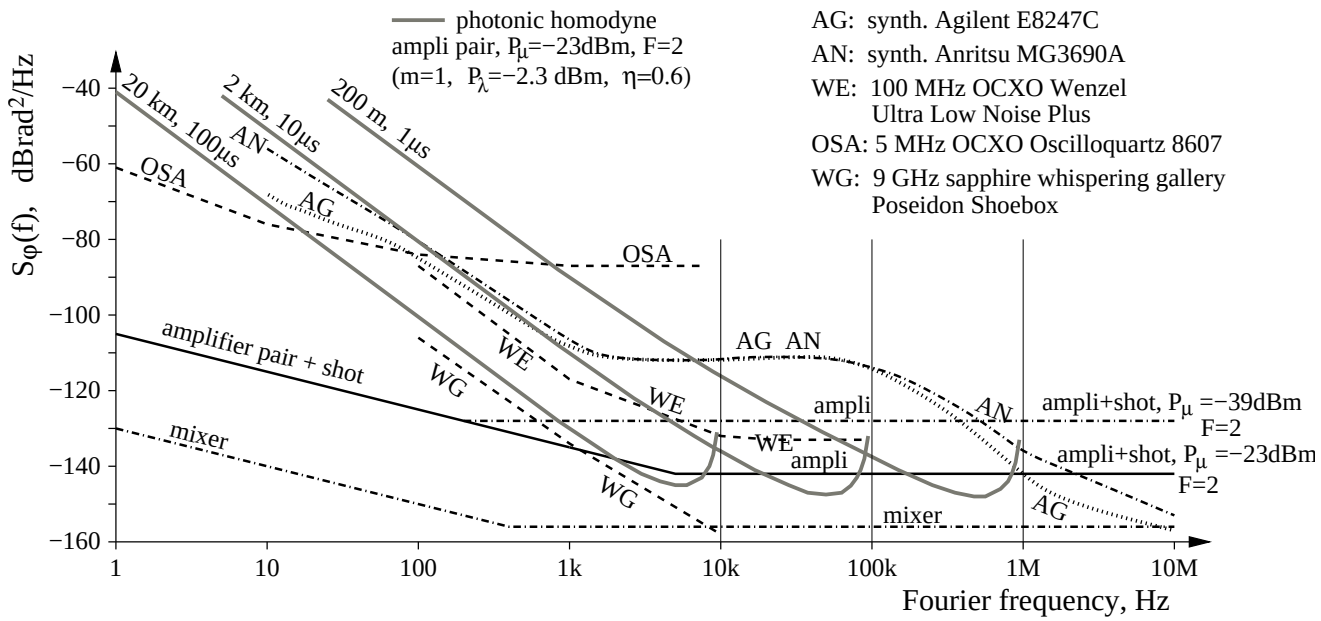

Figure 6. Comparison between phase noise measurement methods. The white noise of the amplifier pair also includes shot noise, calculated from the optical power that gives P_μ with $m = 1$ and $\eta = 0.6$.

1 Hz flicker noise was between 7.4×10^{-13} and 5.9×10^{-11} depending on the detection angle γ. Based on physical insight, we ascribe the maximum to amplitude noise and the minimum to phase noise, that is, 7.4×10^{-13} rad^2/Hz (-121.3 dBrad^2/Hz. These results apply to the measurement of a microwave oscillator, which includes the EOM and the detector (see Fig. 7), and sets the upper bound of the photodetector noise in the measurement of an optical signal. Finally, the flicker noise of the modulator-detector pair is lower by a factor 30 (15 dB) than the noise of the amplifier, thus it does not deserve more attention here.

D. Comparison of Method

Figure 6 compares the phase noise spectrum of some selected low-noise commercially-available sources to the noise of a photonic homodyne instrument. All spectra refer to the carrier frequency of 10 GHz, and to the best low-noise available option. In the case of fixed-frequency oscillators (quartz and sapphire), the spectra are converted to 10 GHz using the intrinsic property of frequency multiplication by a rational number z, that $S_{\varphi\,\mathrm{out}} = z^2 S_{\varphi\,\mathrm{in}}$.

A synthesizer can be directly used as the reference in Fig. 2. In this case, the phase noise of the synthesizer sets the measurement limit. Phase noise can be further reduced in the lower part of the spectrum by locking the synthesizer to an external source. The cutoff frequency below which locking is effective depends on the synthesizer inside.

A quartz oscillator followed by a frequency multiplier can be used as the reference, using the scheme of Fig. 2 B. Experience suggests choosing from 5 MHz and 100 MHz oscillators. The 5 MHz oscillator offer the lowest noise at low f because of the higher Q and of the superior stability of the 5 MHz resonator as compared to the 100 MHz ones. In some cases $\sigma_y(\tau)$ can be lower than 10^{-13} for $\tau \approx 1$ s. On the other hand, white noise is relatively high because the white noise of the internal amplifier is raised by the high order of frequency multiplication (2×10^3) required to attain 10 GHz. 100 MHz oscillators benefit from the lower order of needed multiplication (10^2), and from the lower white noise that results from exciting the resonator at higher power. Yet, the excitation power further reduces the low-frequency stability. Even lower noise can be obtained with a whispering gallery mode reference oscillator, which benefits from the high Q of the resonator. Yet, in that case an oscillator close to the frequency of the source under test is necessary.

The noise limit of the delay-line measurements originates from the noise of its constituent components, chiefly the amplifier pair, converted into input phase noise using Eq. (5) and (6). The white noise of the amplifier pair also include the shot noise. The latter is obtained by deriving P_λ from P_μ. Eq. (12) is used, with $m = 1$ and $\eta = 0.6$. Three cases are considered, in which the line length is 20 km, 2 km, and 200 m. The upper frequency limit comes from $f\tau = 0.95$, where Eq. (5) yields a correction of 16 dB. Between $f = 0.95/\tau$ and $f = 1/\tau$ the output voltage spectrum goes abruptly to zero, where no measurement is possible.

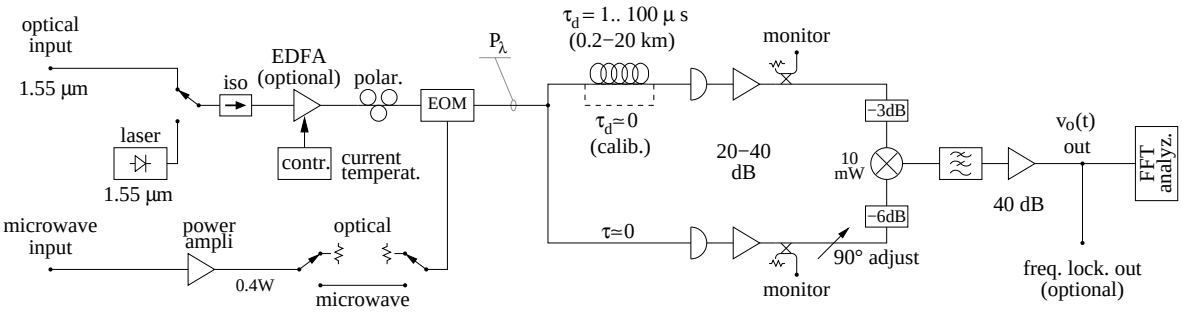

Figure 7. Scheme of the instrument.

5. Measurement of Delay-Line Oscillators

The background noise of the photonic homodyne instrument (Fig. 3 A), for $f \ll 1/2\pi\tau_d$ is approximated by

$$S_{\varphi i}(f) = \left(\frac{1}{2\pi\tau_d}\right)^2 \frac{1}{f^2} S_{\varphi o}(f) \quad , \tag{22}$$

where $S_{\varphi o}(f)$ is the overall phase noise of the optical and electrical part, chiefly the amplifier noise dominant at low f. Eq. (22) is (5) inverted and approximated for low f.

Let us consider a delay-line oscillator at the frequency ν_0. Its phase noise is given by the Leeson formula[31]

$$S_{\varphi l}(f) = \left[1 + \frac{\nu_0^2}{4Q^2}\,\frac{1}{f^2}\right]\, S_{\varphi a}(f) \quad , \tag{23}$$

where $S_{\varphi a}(f)$ is the phase noise of the sustaining amplifier, and more generally the equivalent phase noise of the electronics in the loop. Taking $Q = \pi\nu_0\tau_d'$ as the equivalent merit factor of the delay line that is used as the resonator, and dropping the term "1+" in the square brackets, negligible at low f, (23) becomes

$$S_{\varphi l}(f) = \left(\frac{1}{2\pi\tau_d'}\right)^2 \frac{1}{f^2} S_{\varphi a}(f) \quad . \tag{24}$$

Eq. (24) is formally identical to (22). Hence, at first glance one may believe that the background noise of the instrument is the same as the oscillator noise $[S_{\varphi i}(f) = S_{\varphi l}(f)]$ if the same key components are used. This means $\tau_d = \tau_d'$ for the delay line, and the same phase noise for the amplifier. Yet, the oscillator makes use of one amplifier, while the instrument (Fig. 3 A) needs two amplifiers. Thus, the instrument must have either a superior amplifier technology, or a longer delay line. Of course, a longer line limits the maximum f. On the other hand the design of the instrument, compared to the design of an oscillator, allows more freedom in choosing the most appropriate working point of all parts. Therefore, it is possible to successfully design an instrument based on the same (or similar) delay and amplifier of the oscillator to be measured.

6. Experimental Results

Figure 7 shows the complete measurement scheme. It makes possible the measurement of photonic oscillators, and of traditional microwave oscillators by modulating the internal 1.55 μm optical source. While phase locking is impossible, the oscillator under test can still be frequency-locked to the discriminator. The delay line is a Coreguide SMF28 optical fiber that exhibits an attenuation of 0.2 dB/km and a refractive index of 1.45. Using a 2 km fiber, the delay is $\tau_d = 9.67$ μs. Thus, the first null of $|H_\varphi(f)|^2$ occurs at $f = 103.4$ kHz. The amplifier noise figure F is of about 2.5 (4 dB), which also account for the losses in the detector-amplifier path.

The first experiment is the measurement of a 9.9 GHz microwave source that consists of a 100 MHz quartz oscillator (Wenzel CO 233 VFW) followed by a ×99 frequency multiplier (MATS PLX32-18). The optical power P_λ was set to 1.7 mW, and the modulation index m was close to 1. Under these conditions, Eq. (16) predicts a noise floor of $4{\times}10^{-15}$ rad^2/Hz (-144 dBrad^2/Hz). Yet, P_λ and m tend to drift during the experiment because removing the connectors and reconfiguring the circuit takes some time. This instability, due to microwave induced thermal effects in the EOM, makes the prediction of (16) rather optimistic, by an estimated factor of about two.

Figure 8 shows the results of the first experiment. Setting $\tau_d = 0$ (the delay line is bypassed) we get the curve A, which is the residual noise of the instrument referred at the mixer input. The left part fits $S_\varphi(f) = 4{\times}10^{-11} f^{-1}$ (-104 dBrad^2/Hz at $f = 1$ Hz). This is the phase flicker of the amplifiers. Curve A has a bump at 3 kHz and also at 30 kHz, which hides the white noise floor predicted by (16). This bump is ascribed to the EDFA. Curve B shows the residual noise referred to the oscillator input, which is the instrument limit in the final measurement. It is derived from curve A using Eq. (5). The left part of curve B, from 10 Hz to some 2 kHz, is a frequency flicker of coefficient $b_{-3} = 1.08{\times}10^{-2}$. Curve C is the phase noise of the oscillator, measured with the delay line. This result is fitted by the power-law

$$S_\varphi(f) = \frac{1.1{\times}10^{-2}}{f^3} + \frac{3{\times}10^{-4}}{f^2} + 7.7{\times}10^{-12} \tag{25}$$

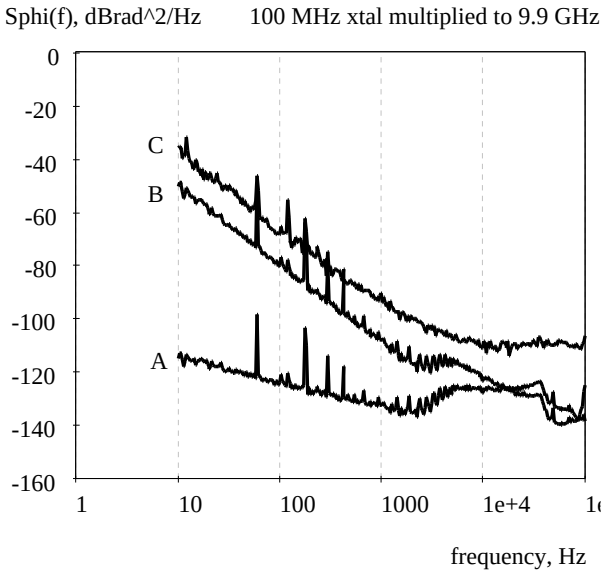

Figure 8. Measurement of a multiplied quartz oscilla

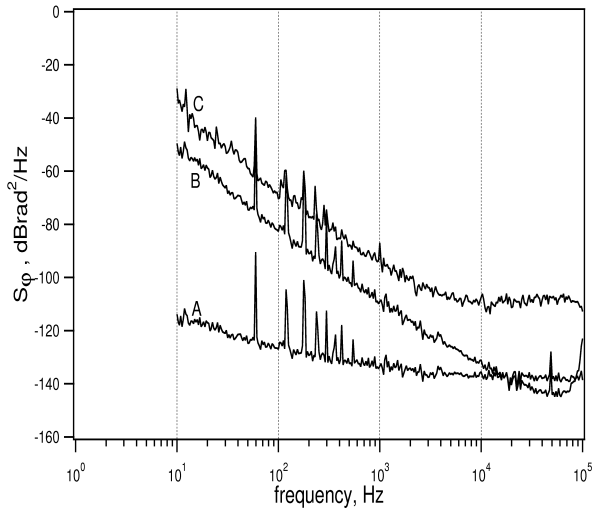

Figure 9. Measurement of the multiplied quartz oscillator of Fig. 8, reproduced with a different experimental configuration.

($b_{-3} = 1.08\times10^{-2} = -7.7$ dBrad^2/Hz, $b_{-2} = 3\times10^{-4} = -35.2$ dBrad^2/Hz, $b_0 = 7.7\times10^{-12} = -111.2$ dBrad^2/Hz). Flicker and white frequency noise originate in the quartz oscillator, while the white phase noise may be due to the oscillator or to the multiplier. The Allan deviation $\sigma_y(\tau)$, calculated with the conversion formulae available in the References 6–10, and discarding the white phase noise, is $\sigma_y = 1.25\times10^{-11}$ for the background noise of the instrument, and

$$\sigma_y(\tau) = 4.9\times10^{-11} + \frac{1.24\times10^{-12}}{\sqrt{\tau}} \qquad (26)$$

for the oscillator under test.

Figure 9 gives an idea of the reproducibility of our

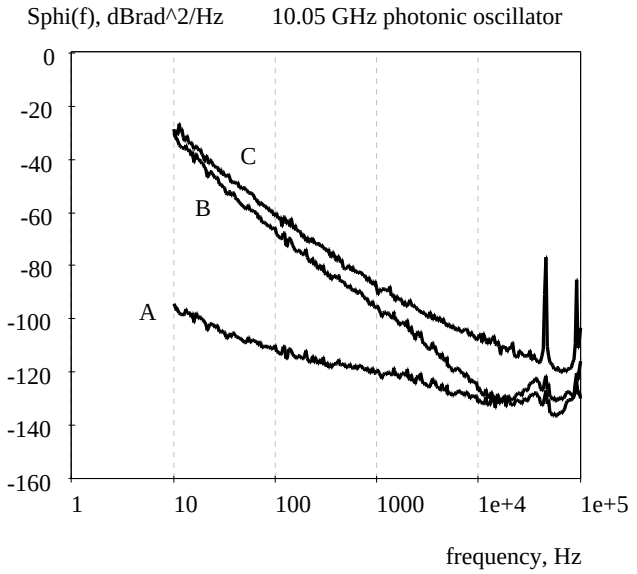

Figure 10. Measurement of a photonic oscillator.

method. This figure refers to the same microwave source of Fig. 8, measured some 6 months later by a different operator after changing some relevant components. The EOM is now a JDS Uniphase MZ-150-120-T-1-1-C2-I2-O2. The laser diode is replaced with a more powerful one (FITEL FOL 15DCWB-A81-19210-B), for the EDFA is no longer necessary. The optical power is $P_\lambda = 1.9$ mW, with a modulation index $m = 0.53$. Curves A, B, and C have the same meaning as in Fig. 8. The bumps at 3 kHz and 30 kHz are now disappeared form curves A and B, while the flicker limit is almost unchanged. After a minimum of smoothing, the oscillator noise (curve C) overlaps to the previous measurement within 0.5 dB.

The second experiment is the measurement of a 10.05 GHz photonic oscillator based on a 4 km optical fiber. The 1.55 μm optical output had to be amplified from the power of 9.5 μW to 1.7 mW with the EDFA. Figure 10 shows the results. Plots A, B, and C have the same meaning and are measured in the same way as before. Curve A fits the $1/f$ line only in the frequency range from 40 Hz to less than 1 kHz, and increases below 40 Hz. The residual flicker is some 5 times (7 dB) higher than in the previous case. We ascribe this otherwise unexplained phenomenon to the amplitude noise of the oscillator, taken in by the mixer. Between 20 Hz and 10 kHz, plot C (oscillator noise) is fitted by the model

$$S_\varphi(f) = \frac{8\times10^{-1}}{f^3} + \frac{1.2\times10^{-3}}{f^2} \qquad (27)$$

($b_{-3} = 0.8 = -1\,\text{dBrad}^2/\text{Hz}$, $b_{-2} = 1.2\times10^{-3} = -29.2\,\text{dBrad}^2/\text{Hz}$), which reveals the presence of flicker and white frequency noise. Below some 20 Hz, the curve C is not representative of the oscillator phase noise because it is raised by the background noise. Converting

the flicker and the white frequency noise into Allan deviation, we get

$$\sigma_y(\tau) = 1\times10^{-10} + \frac{2.4\times10^{-12}}{\sqrt{\tau}} \quad . \tag{28}$$

Finally, we remark that by using a 2 km delay line it has been possible to measure the noise of an oscillator based on a 4 km delay line, making use of similar approach and parts. This supports the conclusion of Sec. 5 that in practice the background noise of the instrument can often be made lower than the oscillator noise, if similar parts are used.

7. Final Remarks

The phase noise measurement method proposed in this paper features simplicity, straightforward implementation, and great flexibility. It is suitable for a wide range of carrier frequency (some 2 octaves, depending on the microwave mixer and amplifiers), it accepts either microwave or modulated optical input, and it does not require phase locking. Additionally, the presence of the optical channel enables EMI isolation, ground isolation, and provides the ultimate shielding. Sensitivity, which is not the main virtue of this method, is indeed high in the 10^2–10^6 Hz region, depending on the delay used in the instrument. For example, using a 20 km optical fiber (see Fig. 6) the background noise calculated in the 10^2–10^3 Hz region is 20 dB lower than the phase noise of microwave synthesizers, and only 5 dB higher than that of the best commercial whispering gallery mode oscillator.

Acknowledgments

The research described in this paper was carried out at the Jet Propulsion Laboratory, California Institute of Technology, under contract of the National Aeronautics and Space Administration, and with support from ARL and AOSP/DARPA. ER was partially supported by the Université Henri Poincaré while visiting JPL.

References

1. X. S. Yao, L. Davis, and L. Maleki, "Coupled optoelectronic oscillators for generating both RF signal and optical pulses," *J. Ligtwave Technology*, vol. 18, pp. 73–78, Jan. 2000.
2. X. S. Yao and L. Maleki, "Optoelectronic microwave oscillator," *J. Optical Society of America B - Optical Physics*, vol. 13, pp. 1725–1735, Aug. 1996.
3. D. J. Jones, K. W. Holman, M. Notcutt, J. Ye, J. Chandalia, L. A. Jiang, E. P. Ippen, and H. Yokoyama, "Ultralow-jitter, 1550-nm modelocked semiconductor laser synchronized to a visible optical frequency standard," *Optics Lett.*, vol. 28, pp. 813–815, May 15 2003.
4. T. A. Yilmaz, C. M. Depriest, A. Braun, J. Abeles, and P. J. Delfyett, "Noise in fundamental and harmonic modelocked semiconductor lasers: Experiments and simulations," *IEEE J. Quantum Electronics*, vol. 39, pp. 838–849, July 2003.
5. S. T. Cundiff and J. Ye, "Colloquium: Femtosecond optical frequency combs," *Review of Modern Physics*, vol. 75, pp. 325–342, Jan. 2003.
6. J. Rutman, "Characterization of phase and frequency instabilities in precision frequency sources: Fifteen years of progress," *Proceedings IEEE*, vol. 66, pp. 1048–1075, Sept. 1978.
7. CCIR Study Group VII, "Characterization of frequency and phase noise, Report no. 580-3," in *Standard Frequencies and Time Signals*, vol. VII (annex) of *Recommendations and Reports of the CCIR*, pp. 160–171, Geneva, Switzerland: International Telecommunication Union (ITU), 1990.
8. V. F. Kroupa, ed., *Frequency Stability: Fundamentals and Measurement.* New York: IEEE Press, 1983.
9. J. Vanier and C. Audoin, *The Quantum Physics of Atomic Frequency Standards*, vol. 2 vol. Bristol: Adam Hilger, 1989.
10. J. R. Vig (chair.), *IEEE Standard Definitions of Physical Quantities for Fundamental Frequency and Time Metrology–Random Instabilities (IEEE Standard 1139-1999).* IEEE, New York, 1999.
11. M. H. Hines, J. Claude R. Collinet, and J. G. Ondria, "FM noise suppression of an injection phase-locked oscillator," *IEEE Transactions on Microwave Theory and Techniques*, vol. 16, pp. 738–742, Sept. 1968.
12. K. Kurokawa, "Noise in synchronized oscillators," *IEEE Transactions on Microwave Theory and Techniques*, vol. 16, pp. 234–240, Apr. 1968.
13. P.-Y. Bourgeois, Y. Kersalé, N. Bazin, M. Chaubet, and V. Giordano, "Cryogenic open-cavity sapphir resonator for ultra-stable oscillator," *Electronics Letters*, vol. 39, pp. 780–781, May 15 2003.
14. G. J. Dick and R. T. Wang, "Stability and phase noise tests of two cryo-cooled sapphire oscillators," *IEEE Transactions on Ultrasononics, Ferroelectrics and Frequency Control*, vol. 47, pp. 1098–1101, Sept. 2000.
15. R. A. Woode, M. E. Tobar, E. N. Ivanov, and D. Blair, "An ultra low noise microwave oscillator based on high q liquid nitrogen cooled sapphyre resonator," *IEEE Transactions on Ultrasononics, Ferroelectrics and Frequency Control*, vol. 43, pp. 936–941, Sept. 1996.
16. R. A. Campbell, "Stability measurement techniques in the frequency domain," in *Proc. IEEE-NASA Symposium on Short Term Frequency Stability*, (Greenbelt, MD, USA), pp. 231–235, Nov. 23-24 1964.
17. J. G. Ondria, "A microwave system for the measurement of AM and PM noise spectra," *IEEE Transactions on Microwave Theory and Techniques*, vol. 16, pp. 767–781, Sept. 1968.
18. A. L. Withwell and N. Williams, "A new microwave

technique for determining noise spectra at frequencies close to the carrier," *Microwave Journal*, vol. 2, pp. 27–32, Nov. 1959.
19. R. V. Pound, "Electronic frequency stabilization of microwave oscillators," *Review of Scientific Instruments*, vol. 17, pp. 490–505, Nov. 1946.
20. F. Labaar, "New discriminator boosts phase noise testing," *Microwaves*, vol. 21, pp. 65–69, Mar. 1982.
21. A. L. Lance, W. D. Seal, and F. Labaar, "Phase noise and AM noise measurements in the frequency domain," in *Infrared and Millimeter Waves* (K. J. Button, ed.), vol. 11, pp. 239–284, Academic Press, 1984.
22. D. Halford, A. E. Wainwright, and J. A. Barnes, "Flicker noise of phase in RF amplifiers: Characterization, cause, and cure," in *Proc. Frequency Control Symposium*, pp. 340–341, Apr. 22–24, 1968. Abstract only is published.
23. A. Hati, D. Howe, D. Walker, and F. Walls, "Noise figure vs. PM noise measurements: A study at microwave frequencies," in *Proc. European Frequency and Time Forum & Frequency Control Symposium Joint Meeeting*, May 5–8, 2003.
24. F. L. Walls, E. S. Ferre-Pikal, and S. R. Jefferts, "Origin of $1/f$ PM and AM noise in bipolar junction transistor amplifiers," *IEEE Transactions on Ultrasononics, Ferroelectrics and Frequency Control*, vol. 44, pp. 326–334, Mar. 1997.
25. E. Rubiola, E. Salik, N. Yu, and L. Maleki, "Phase noise measurement of low power signals," *Electronics Letters*, vol. 39, pp. 1389–1390, sep 18, 2003.
26. E. Rubiola and V. Giordano, "Advanced interferometric phase and amplitude noise measurements," *Review of Scientific Instruments*, vol. 73, pp. 2445–2457, June 2002.
27. X. S. Yao and L. Maleki, "Multiloop optoelectronic oscillator," *IEEE J. Quantum Electronics*, vol. 36, pp. 79–84, Jan. 2000.
28. R. Brendel, G. Marianneau, and J. Ubersfeld, "Phase and amplitude modulation effects in a phase detector using an incorrectly balanced mixer," *IEEE Transactions on Instrumentation and Measurement*, vol. 26, pp. 98–102, June 1977.
29. G. Cibiel, M. Régis, E. Tournier, and O. Llopis, "AM noise impact on low level phase noise measurements," *IEEE Transactions on Ultrasononics, Ferroelectrics and Frequency Control*, vol. 49, pp. 784–788, June 2002.
30. W. Shieh, X. S. Yao, L. Maleki, and G. Lutes, "Phase-noise chracterization of optoelectronic components by carrier suppression techniques," in *Digest of the Optical Fiber Communications Conference*, (San José, CA), pp. 263–264, May 23-25 1998.
31. D. B. Leeson, "A simple model of feed back oscillator noise spectrum," *Proceedings IEEE*, vol. 54, pp. 329–330, Feb. 1966.